# 3DOP: Comfort-oriented Motion Planning for Automated Vehicles with Active Suspensions

Yanggu Zheng[1], Barys Shyrokau[1] and Tamas Keviczky[2]

***Abstract*— Motion comfort is the basis of many societal benefits promised by automated driving and motion planning is primarily responsible for this. By planning the spatial trajectory and the velocity profile, motion planners can significantly enhance motion comfort, ideally without sacrificing time efficiency. Active suspensions can push the boundary further by enabling additional degrees of freedom in the controllable vehicle motions. In this paper, we propose to integrate the planning of roll motion into an optimization-based motion planning algorithm called 3DOP (3 Degrees-of-Freedom Optimal Planning), where the conflicting objectives of comfort and time efficiency are optimized. The feasibility of the planned motion is verified in a realistic simulation environment, where feedforward-proportional control suffices to track the speed, path, and roll references. The proposed scheme achieves a significant reduction of motion discomfort, namely by up to 28.1% over the variant without controllable roll motion, or up to 34.2% over an acceleration-bounded driver model. The results suggest a considerable potential of improving motion comfort by equipping automated vehicles with active suspensions.**

## I. INTRODUCTION

Automated driving is steadily becoming a reality. The occupants behind the steering wheel, if there still is one, can be freed conditionally from observing, planning, and acting. But looking at handheld displays means the loss of external visual cues on the vehicle's motion, which magnifies visual-vestibular conflict when the vehicle changes speed or negotiates turns. The occupants hence become prone to motion sickness, which in return reduces their willingness and performance in activities that require visual attention [1]. The paradoxical situation can be effectively eased by reducing the disturbances that passengers are subjected to. In automated vehicles, such responsibility falls primarily on the motion planner. A large variety of algorithms considers the comfort aspect of vehicle motion [2]. Guaranteeing smoothness of the spatial path was a primary focus in early studies. Parametric curves including Clothoids [3], Bezier curves [4], and splines [5] have been used frequently. The attention to smoothness can also be found when generating velocity profiles [6] that is effectively motion planning in 1-dimensional space. The research interest shifted later to the mitigation of motion sickness. The low-frequency translational accelerations are considered to be the main contributor to motion sickness [7] [8]. Motion primitives generated with bounded acceleration were used in combination with the Rapidly-exploring Random Tree (RRT) algorithm to explore unstructured free space [9], but the results were not satisfactory. Several studies chose the minimization of translational accelerations as the objective while including travel time in the evaluation of a motion plan [10]–[12]. Such approaches are more commonly used for structured roads.

Motion planning is not the only solution to enhancing motion comfort. For example, the steering control has been given the freedom to locally deviate from the planned path if needed and therefore reduces lateral acceleration [13]. Active suspensions can also have an impact on motion comfort. In addition to the traditional role of filtering out road unevenness, they allow manipulation of the vehicle attitude. Passive roll rotation of the vehicle body amplifies the lateral acceleration sensed by the occupants. It projects the gravity along the occupant's local horizontal plane, in the same direction as the centripetal acceleration. The impact is measured as approximately $0.17\,\mathrm{m/s^2/deg}$ across the permissible range of roll motion on most passenger vehicles. Naturally, vehicles with a higher center of gravity and softer suspensions are more susceptible to this impact. With active suspensions, gravity can be exploited in the opposite direction by tilting the vehicle body against the centripetal force. The concept is commonly known as curve tilting and was first applied on railroad vehicles [14] before it appeared on passenger vehicles later [15]. However, with a human driver in the control loop, the effectiveness of curve tilting is limited: The reference roll motion is generated conservatively, based on curvature preview [16] [17]. The suspension controller faces unpredictable disturbances induced by the driver which are harmful to the control quality. These problems could potentially be resolved by the presence of a motion planner on an automated vehicle. In this case, the curve tilting function no longer has to match the driver's anticipation or react to driver inputs. As an immediate benefit, the motion planning information can help improve the control quality by providing an accurate forecast of the disturbance. Further improvement of motion comfort may be achieved by coordinating the roll motion with the planar motion.

The contribution of this paper is a motion planning algorithm that optimizes motion comfort and time efficiency by jointly planning the path, velocity, and roll of an automated vehicle equipped with active suspensions. The algorithm is explained in detail in Section II. Section III introduces the

The research leading to these results has received funding from the European Union Horizon 2020 Framework Program, Marie Sklodowska-Curie actions, under grant agreement no. 872907.

[1]Yanggu Zheng and Barys Shyrokau are with the Department of Cognitive Robotics, Faculty of Mechanical, Maritime and Materials Engineering, Delft University of Technology, 2628CD, The Netherlands y.zheng-2@tudelft.nl, b.shyrokau@tudelft.nl

[2]Tamas Keviczky is with Delft Center for Systems and Control, Faculty of Mechanical, Maritime and Materials Engineering, Delft University of Technology, 2628CD, The Netherlands t.keviczky@tudelft.nl

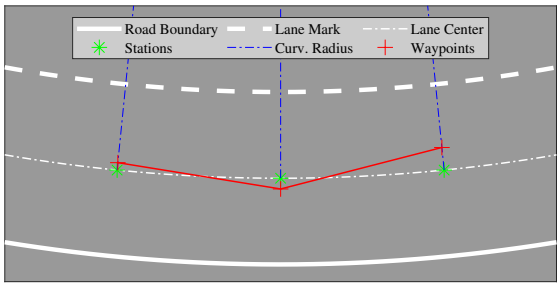


Fig. 1. A visual explanation of the definition of stations and waypoints on a road section with right-hand traffic.

virtual environment and corresponding motion control setups used to test the algorithm, in addition to the baseline methods to compare with. The results are presented in Section IV and Section V summarizes the findings of this study and indicates future directions.

## II. Optimal Motion Planning

### A. Motion Definition

The proposed planning algorithm, referred to as '3DOP', considers the planar and roll motion of the vehicle. It outputs desired vehicle motions that are defined through the available driving space on well-paved roads and are to be fulfilled by chassis actuators and controllers. The road profile consists of consecutive sectors, each assigned with a curvature and a length. The sectors are further discretized into a string of reference stations distributed along the lane center. At each station, a local lateral axis is defined along the curvature radius, with the left-hand side of the driving direction being positive. The vehicle's path is then constructed with a set of waypoints (Fig. 1), each located relative to the corresponding station with a lateral position $y$. The velocity $v$ and roll angle $\phi$ of the vehicle when passing a waypoint are directly assigned by the motion planner and the accelerations are calculated accordingly.

### B. Objective Function

The purpose of 3DOP is to improve comfort while preserving time efficiency for passengers traveling on an automated vehicle. We choose to minimize the weighted sum of discomfort and maneuver time:

$$J = W_{\text{time}} T + D \tag{1}$$

Where a relative weighting factor $W_{\text{time}}$ is used for maneuver time $T$ and is varied to cover a wide spectrum of user preferences. A small weight suits those who are highly susceptible to motion sickness, whereas a larger weight can be selected by those in an urgent transit. Although maneuver time is straightforward to calculate, comfort is a more abstract concept to measure. We choose to characterize the major discomfort indicator in (2), as the integral of squared accelerations along the passenger's perceived horizontal plane. In this way, the effect of vehicle body tilt on the lateral acceleration sensed by the passenger is incorporated. It differs from the motion sickness dose value (MSDV) used in [11]. It remains uncertain whether the MSDV concept could be generalized to combined longitudinal and lateral accelerations whereas the computation of relative quantities increases the complexity of the problem.

$$D_{\text{acc}} = \int_0^T \left(a_x^2 + a_y^2\right) dt \tag{2}$$

The controlled roll motion, on the other hand, is an additional source of discomfort that should not be neglected. Human experiments suggest a perception threshold of $0.5\,\mathrm{deg/s}$ for the frequency component of $1\,\mathrm{Hz}$ [18]. This is far below the roll rate observed on curve tilting systems [17], meaning that the roll motion could be perceived in most situations. Hence, we penalize the absolute roll motion in an additional roll-related discomfort term (3). The total discomfort is then given by (4), which is the sum of acceleration-related discomfort and roll-related discomfort scaled with weighting factor $W_{\text{roll}}$.

$$D_{\text{roll}} = \int_0^T \left|\dot{\phi}\right| dt \tag{3}$$

$$D = D_{\text{acc}} + W_{\text{roll}} D_{\text{roll}} \tag{4}$$

The entire motion consists of $M = N - 1$ segments connecting 2 adjacent waypoints, with $N$ being the total number of waypoints. The integral form of the objective function is equivalent to the sum of segment values:

$$J = \sum_{k=1}^{M} \left(W_{\text{time}} \Delta T_k + \Delta D_{\text{acc},k} + W_{\text{roll}} \Delta D_{\text{roll},k}\right) \tag{5}$$

The segment values are calculated as:

$$\begin{aligned} \Delta D_{\text{acc},k} &= \textstyle\int_{T_k}^{T_{k+1}} \left(a_{x,k}^2 + a_{y,k}^2\right) dt \\ \Delta D_{\text{roll},k} &= \textstyle\int_{T_k}^{T_{k+1}} \left|\dot{\phi}\right| dt \end{aligned} \tag{6}$$

Within a segment, we consider the velocity and roll angle to change linearly with respect to time. Knowing the distance between the two waypoints $d_k$ ($1\,\mathrm{m}$ in our case) gives the following:

$$\begin{aligned} \Delta T &= \tfrac{2 d_k}{v_k + v_{k+1}} \\ a_{x,k} &= (v_{k+1} - v_k)/\Delta T \\ \dot{\phi}_k &= (\phi_{k+1} - \phi_k)/\Delta T \end{aligned} \tag{7}$$

Further, we assume the curvature remains constant within the segment, calculated as:

$$\kappa_k = (\psi_{k+1} - \psi_k)/d_k \tag{8}$$

The lateral acceleration within the segment is hence approximated as:

$$\begin{aligned} a_{y,k} &= \kappa_k \bar{v}_k^2 - g \sin \bar{\phi}_k \\ \bar{v}_k &= (v_k + v_{k+1})/2 \\ \bar{\phi}_k &= (\phi_k + \phi_{k+1})/2 \end{aligned} \tag{9}$$

Combining these equations allows to determine the value of $J$ from a given motion plan.

### C. Constraints and Initialization

The comfort vs time-efficiency optimization produces reasonable results only when constrained properly. In our case, box constraints are placed on all motion variables. For lateral position, the bounds are determined by the width of the lane and the vehicle body. A typical lane width of $3.75\,\mathrm{m}$ is found in most European countries, outside populated areas. A representative width of a D-segment passenger vehicle including mirrors is under $2.10\,\mathrm{m}$. Hence the vehicle is allowed to deviate from the lane center by up to $0.75\,\mathrm{m}$ on each side and the remaining centimeters are left as a safety margin. The vehicle's forward velocity is constrained according to local policies. In the Netherlands, a speed limit of $80\,\mathrm{km/h}$ is found on most distributor (rural) roads. The roll angle of the vehicle body is constrained to lie between $\pm\,5\,\mathrm{deg}$. Given a track width of $1.6\,\mathrm{m}$, an active suspension actuator is required to lift or lower the vehicle body on its side by $7\,\mathrm{cm}$. Furthermore, the vehicle is expected to drive along the lane center at the speed limit when entering and exiting the scenario (see Section III-A), from and into road sectors with negligible bending. Hence the lateral position of the first and the last waypoint is 0, velocity $80\,\mathrm{km/h}$. This ensures an acceptable behavior for the vehicles behind and on the adjacent lanes. No additional measure is taken to ensure feasibility of the planned motion concerning vehicle dynamics. The aggressiveness of the motion has to be far below friction limit to be considered comfortable by the passengers. This ensures that the performance is only directly influenced by the choice of weights in the cost function and not by the tightness of additional constraints. It is still possible to maintain a safety margin at low-friction conditions by only allowing a very small $W_{\text{time}}$.

### D. Optimization Problem and Solver

The motion plan consisting of $3N$ decision variables is determined by solving the optimization problem formulated as (10). For this purpose, we used the Sequential Quadratic Programming (SQP) algorithm in MATLAB R2020b. The step tolerance was reduced to $10^{-10}$ while the other parameters remain as default.

$$\begin{aligned} \text{min:} \quad & J(\mathbf{X}) \\ \text{where:} \quad & \mathbf{X} = [y_1 \dots y_N, v_1 \dots v_N, \phi_1 \dots \phi_N] \\ \text{s.t.:} \quad & y_{\min} \le y_1 \dots y_N \le y_{\max} \\ & v_{\min} \le v_1 \dots v_N \le v_{\max} \\ & \phi_{\min} \le \phi_1 \dots \phi_N \le \phi_{\max} \end{aligned} \tag{10}$$

## III. Testing Method

### A. Scenario and Simulation Setup

The proposed method is tested under a scenario where comprehensive and intensive control of the vehicle is required. We choose here a transitional section of a real road that exists in the Netherlands. The vehicle enters the scenario from the exit ramp of motorway A12 (52.064° N, 4.818° E), passes two roundabouts plus the consecutive turns in between, and departs through distributor road N420 (52.068° N, 4.828° E). The road section has a nominal length of $520\,\mathrm{m}$, involving 9 turns of different radii and angles in total. The motion planner processes the road information to determine the optimal motion. The feasibility of the planned motion is then tested using a validated multi-body vehicle model in the virtual testing platform IPG CarMaker. An identical road section is constructed inside the software. The virtual vehicle is expected to navigate through the road section while following the planned motion with the help of basic controllers described in Section III-B.

### B. Motion Control

Three feedforward proportional controllers are set up for executing the planned motion, each responsible for one specific motion regime. For path following, a Stanley controller in the simplified form of (11) is implemented. This method shows sufficient path tracking performance under normal driving conditions compared to its state-of-the-art counterparts [19]. The steering angle of the front wheels accounts for heading and lateral positional error. The tuning parameter $k_{\text{steer}}$ regulates the aggressiveness of corrections to the lateral error.

$$\delta = (\psi_r - \psi) + \arctan \frac{k_{\text{steer}}\,(y_r - y)}{v} \tag{11}$$

The speed control is governed by (12) and gives throttle and brake percentage, $P_{\text{T}}$ and $P_{\text{B}}$, as control inputs. The desired acceleration is calculated as the sum of the forward acceleration derived from the motion plan, $a_{x,r}$, and the velocity tracking error scaled by $k_{\text{speed}}$. Then the desired acceleration is scaled by $k_{\text{drive}}$ or $k_{\text{brake}}$ to find the pedal input, depending on the sign of the desired acceleration: throttle for positive and brake for negative.

$$\begin{aligned} P_{\text{T}} &= k_{\text{drive}}\,(a_{x,r} + k_{\text{speed}}\,(v_r - v)) \times 100\% \\ P_{\text{B}} &= k_{\text{brake}}\,(a_{x,r} + k_{\text{speed}}\,(v_r - v)) \times 100\% \end{aligned} \tag{12}$$

Similarly, the roll angle control utilizes the lateral acceleration derived from the motion plan to construct a feedforward input. The roll moment exerted by the centripetal acceleration is compensated for accordingly. Another feedforward term is based on suspension characteristics. The vehicle body's natural roll stiffness means a roll moment always exists in the opposite direction of the roll motion, which also should be balanced out. Then, the correction of the roll angle is handled by a proportional term. The total roll moment the active suspensions should generate is given by (13) and is distributed among the actuators according to (14).

$$M_{\text{roll}} = M_{\text{acc}} + M_{\text{spr}} + k_{\text{roll}}\,(\phi_r - \phi) \tag{13}$$

$$\begin{aligned} F_{z,\text{FL}} &= -F_{z,\text{FR}} = \frac{k_{\phi,\text{F}}}{k_{\phi,\text{F}} + \phi,\text{F}} M_{\text{roll}} \\ F_{z,\text{RL}} &= -F_{z,\text{RR}} = \frac{k_{\phi,\text{R}}}{k_{\phi,\text{F}} + \phi,\text{F}} M_{\text{roll}} \end{aligned} \tag{14}$$

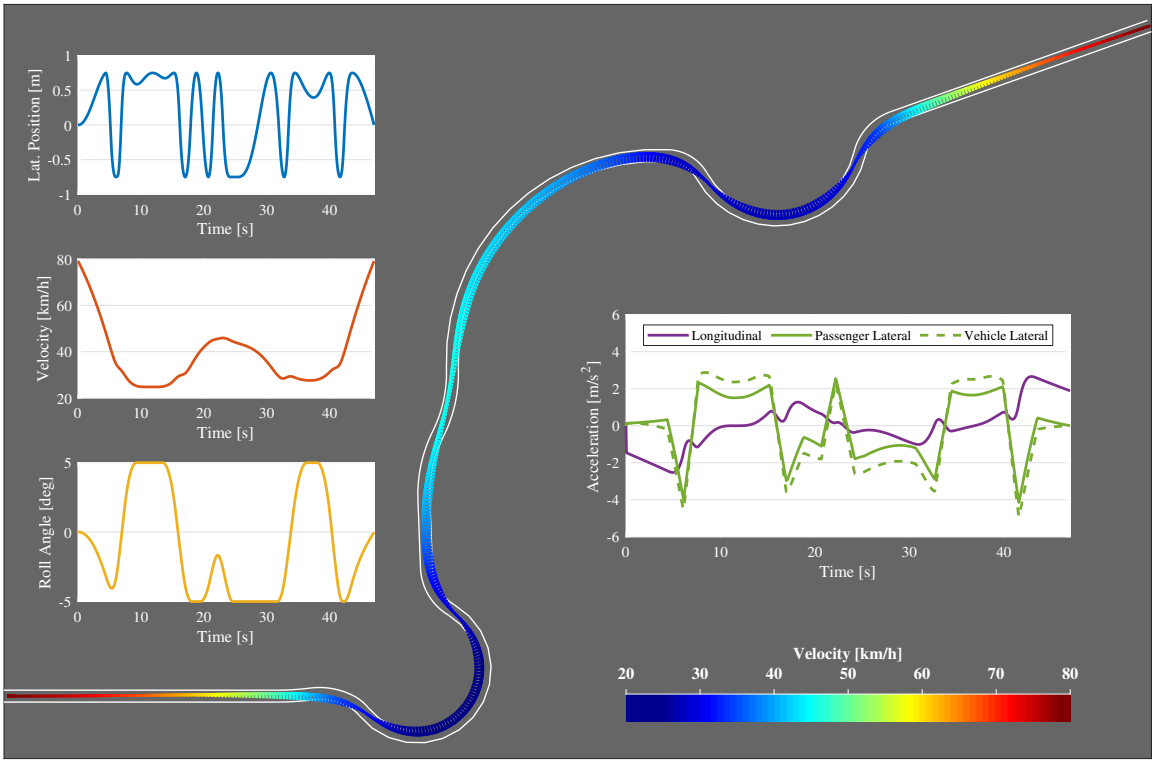


Fig. 2. An optimal motion plan generated with $W_{\text{time}} = 12$. The main figure visualizes the vehicle's ideal motion to navigate through the scenario. The left subfigures show the plans for the lateral position, velocity, and roll angle. The resulting acceleration profile is shown in the subfigure on the right. The green solid line represents the lateral acceleration experienced by the passenger and the green dash line represents the lateral acceleration exerted on the vehicle body. This motion plan has a duration of 47.0 seconds and a discomfort rating of 205.9.

### C. Baselines for Comparison

The benefit of controlling an extra motion DOF is demonstrated by including two reduced-DOF variants of the optimization-based motion planning algorithm: speed-only planning and speed+path planning. In the speed-only case, the vehicle follows the lane center, while in speed+path planning the vehicle can adjust its position to reduce trajectory curvature. In these two cases, the penalty term on roll-related discomfort becomes irrelevant and is hence dropped. We further include an artificial driver model (ADM) provided in IPG CarMaker as an additional baseline method. This driver model is considered to have close-to-optimal performance [20] and hence could represent the performance of highly experienced human drivers. Given certain road geometry and route, the ADM plans the path and speed profile for the vehicle according to acceleration limits and other parameters and controls the vehicle to execute the desired motion. We determined these acceleration limits based on what is observed from 3DOP to ensure a fair comparison.

## IV. Results

### A. An Example of Planned Motion

Fig. 2 presents the motion plan generated with the weighting factor $W_{\text{time}} = 12$. The optimal solution consists of 1557 decision variables, found after 1129 SQP iterations and the cost function was evaluated approximately 1.8M times. The total computation time is 3066 s on a desktop computer with an Intel Core i5-9400F CPU. The optimization was terminated as the stopping criterion of step tolerance $10^{-10}$ had been met. The planner comprehensively utilizes the available lane space and the vehicle's roll capability to reduce lateral acceleration while coordinating the longitudinal velocity. The manner of space utilization highly resembles the racing line used in motorsport where the path curvature should be minimal. Velocity is adjusted in accordance with the curvature. The vehicle slows down prior to sharp turns and accelerates when the path bending is lower. The speed in the middle sector (20-30s) ranges from 30-45 km/h, reflective of real world values observed while actually driving on the site. The corner tilting capability is exploited in a restrained fashion thanks to the additional penalty term. The roll angle, visualized as a row of comb teeth perpendicular to the vehicle path in Fig. 2, does not necessarily follow the vehicle's turning direction. During the right-left-right turns between the two roundabouts, the vehicle only rolls to the right. Because the left turn is relatively short-lasting, changing the roll angle for it would harm comfort through the longer right turns. In the roundabouts, however, the three turns contribute almost equally to acceleration discomfort. The roll angle hence has to change its direction accordingly for minimizing the perceived lateral acceleration. The effect of curve tilting on minimizing passenger-perceived lateral acceleration is obvious from the sub-figure on the right. A reduction of approximately $0.8\,\mathrm{m/s^2}$ is observed when the roll angle is

TABLE I

CONTROL QUALITY OF TRACKING THE MOTION PLAN

| Tracking Error | Position [$10^{-1}$m] | Velocity[km/h] | Roll [deg] |
|---|---|---|---|
| Max Absolute | 1.331 | 0.895 | 0.394 |
| Root-Mean-Square | 0.535 | 0.258 | 0.122 |

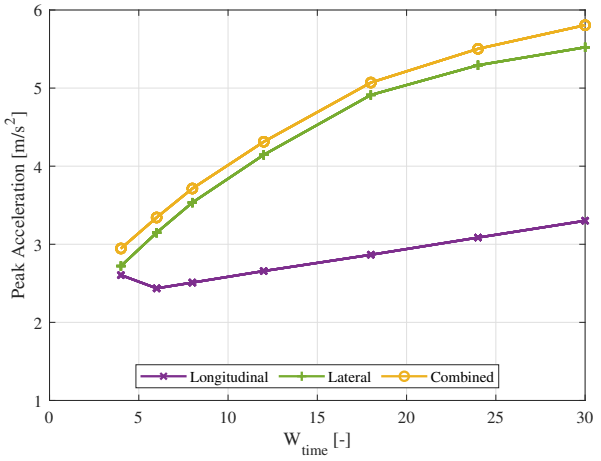


Fig. 3. Variation of peak acceleration magnitude of the planned motions.

commanded to the full. Performing the planned motion in the simulation environment yields tracking errors as given in TABLE I. The values suggest good feasibility of the motion planned by 3DOP.

### B. Peak Accelerations

The peak acceleration of each motion plan is collected in Fig. 3. As $W_{\text{time}}$ increases, the maximum magnitude of lateral acceleration grows as expected. However, the longitudinal acceleration reaches a minimum at $W_{\text{time}} = 6$ before the monotonic upward trend that is observable in lateral acceleration. This is partly due to the length of the entry and exit straights. The smaller lateral acceleration comes at the cost of more change in longitudinal velocity, which has to happen within a limited distance. With $W_{\text{time}}$ under 6, the benefit of reduced lateral acceleration outweighs the cost of increased longitudinal acceleration and the loss of time. The peaks of longitudinal and lateral accelerations are staggered so that the combined planar acceleration is below $5.81\,\text{m/s}^2$ or $0.59\,g$ at the largest $W_{\text{time}}$. This value implies that the motion plans can be performed by most passenger vehicles on dry roads.

### C. Comparison of Performance

We performed simulation runs using the ADM with various acceleration limits derived from Fig. 3. The performance indicators obtained from these runs are shown in Fig. 4. We calculate the weighted sum of time and discomfort of these points to locate the points lying the closest to the lower-left corner. These points represent the best performance of the ADM, effectively forming an approximate Pareto front. The road profile is processed separately by the speed-only and speed+path planning method using the same set of $W_{\text{time}}$.

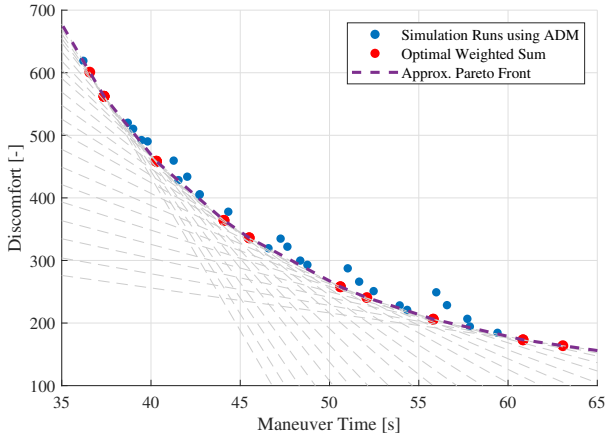


Fig. 4. Performance of the artificial driver model. The settings with the minimal weighted sum of time and discomfort are marked in red. The dashed line segments connecting them form an approximate Pareto front representing the best performance achievable with the driver model.

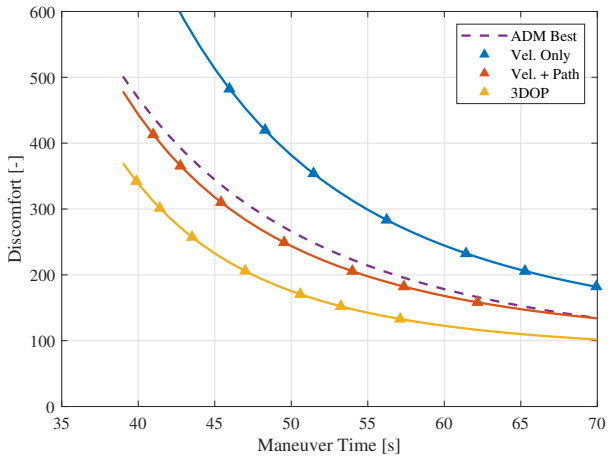


Fig. 5. Comparison of the performance indicators between 3DOP and the baseline planners.

The comparison between 3DOP and these baseline methods is shown in Fig. 5. The string of two-fold scores are fitted as functions in the form of:

$$y = ax^b + c \tag{15}$$

which preserves the trend of increased emphasis on time efficiency accelerates the deterioration of comfort. The improvement of 3DOP over the baseline methods is illustrated in two different ways. Fig. 6 shows the potential gain in motion comfort without losing time efficiency, and the potential savings in travel time with the same comfort level. Across the overlapping range of maneuver time, 3DOP achieves a maximum reduction of discomfort by 54.7% over optimal speed planning, 34.2% over the ADM, or 28.1% over optimal planar motion planning. Alternatively, it saves maneuver time by a maximum of 29.4%, 17.2%, and 14.3% over the three baselines. The time-saving advantage is more obvious when a high level of comfort is demanded because of the limited capability to roll the vehicle body. A higher amplitude of

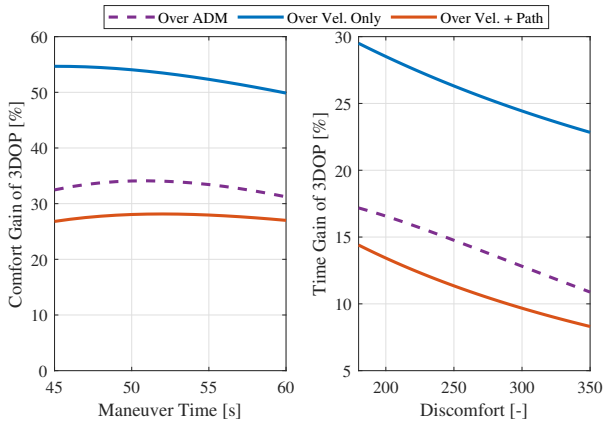


Fig. 6. Advantages of 3DOP over baseline methods.

lateral acceleration means the reduction is smaller in terms of proportion.

## V. Conclusions

### A. Contributions

We presented a motion planning method that jointly plans the path, speed, and roll motion of a vehicle equipped with active suspensions. The method exploits the possibility to actively roll the vehicle body, in order to further improve motion comfort as well as time efficiency. The planned motion is shown to be feasible as it can be tracked by a virtual passenger vehicle with limited error, even when using basic control structures. The results support the use of active suspensions on automated vehicles as the coordination between planar and roll motion can significantly enhance motion comfort. Compared with only optimizing within the horizontal plane, the proposed method improves comfort by up to 28.1% while consuming the same amount of time, or saves at most 14.4% of travel time while maintaining the same level of comfort. The advantage becomes more significant when compared with a driver model representative of highly experienced human drivers.

### B. Limitations and Future Works

We are aware of certain limitations in the current work and plan to deepen the understanding with follow-up studies. Firstly, solving the optimization problem for the entire scenario demands intensive computational effort. This approach cannot be implemented directly as a real-time motion planner. Receding-horizon and data-based approaches could be explored to simplify online computation. Meanwhile, although the objective benefit of the proposed method is attractive, it remains uncertain whether the computed motion profiles are appreciated by users. This question could be answered by subjecting human participants to the planned motions and requesting subjective evaluations from them. Experimental studies can also be exploited to collect human driving data that replaces the parameterized driver model. This will serve better as a baseline that motion planning methods can be compared with. A quantified advantage over human drivers along with verified user acceptance could help promote automated driving to the public.

## References


[1] P. Matsangas, M. E. McCauley, and W. Becker, "The effect of mild motion sickness and sopite syndrome on multitasking cognitive performance," *Human factors*, vol. 56, no. 6, pp. 1124–1135, 2014.

[2] B. Paden, M. Čáp, S. Z. Yong, D. Yershov, and E. Frazzoli, "A survey of motion planning and control techniques for self-driving urban vehicles," *IEEE Transactions on intelligent vehicles*, vol. 1, no. 1, pp. 33–55, 2016.

[3] D. H. Shin, S. Singh, and W. Whittaker, "Path generation for a robot vehicle using composite clothoid segments," *IFAC Proceedings Volumes*, vol. 25, no. 6, pp. 443–448, 1992.

[4] L. Han, H. Yashiro, H. T. N. Nejad, Q. H. Do, and S. Mita, "Bezier curve based path planning for autonomous vehicle in urban environment," in *2010 IEEE intelligent vehicles symposium*. IEEE, 2010, pp. 1036–1042.

[5] T. Berglund, A. Brodnik, H. Jonsson, M. Staffanson, and I. Soderkvist, "Planning smooth and obstacle-avoiding b-spline paths for autonomous mining vehicles," *IEEE Transactions on Automation Science and Engineering*, vol. 7, no. 1, pp. 167–172, 2009.

[6] A. Artuñedo, J. Villagra, and J. Godoy, "Jerk-limited time-optimal speed planning for arbitrary paths," *IEEE Transactions on Intelligent Transportation Systems*, pp. 1–15, 2021.

[7] B. E. Donohew and M. J. Griffin, "Motion sickness: effect of the frequency of lateral oscillation," *Aviation, Space, and Environmental Medicine*, vol. 75, no. 8, pp. 649–656, 2004.

[8] T. Irmak, D. M. Pool, and R. Happee, "Objective and subjective responses to motion sickness: the group and the individual," *Experimental Brain Research*, vol. 239, no. 2, pp. 515–531, 2021.

[9] M. Mischinger, M. Rudigier, P. Wimmer, and A. Kerschbaumer, "Towards comfort-optimal trajectory planning and control," *Vehicle System Dynamics*, pp. 1108–1125, 2018.

[10] H. Shin, D. Kim, and S.-E. Yoon, "Kinodynamic comfort trajectory planning for car-like robots," in *2018 IEEE/RSJ International Conference on Intelligent Robots and Systems (IROS)*. IEEE, 2018, pp. 6532–6539.

[11] Z. Htike, G. Papaioannou, E. Siampis, E. Velenis, and S. Longo, "Minimisation of motion sickness in autonomous vehicles," in *2020 IEEE Intelligent Vehicles Symposium (IV)*. IEEE, pp. 1135–1140.

[12] Y. Zheng, B. Shyrokau, and T. Keviczky, "Comfort and time efficiency: A roundabout case study," in *2021 IEEE International Intelligent Transportation Systems Conference (ITSC)*. IEEE, 2021, pp. 3877–3883.

[13] H. Wang, B. Liu, X. Ping, and Q. An, "Path tracking control for autonomous vehicles based on an improved mpc," *IEEE Access*, vol. 7, pp. 161 064–161 073, 2019.

[14] H. Harris, E. Schmid, and R. Smith, "Introduction: Theory of tilting train behaviour," *Proceedings of the Institution of Mechanical Engineers, Part F: Journal of Rail and Rapid Transit*, vol. 212, no. 1, pp. 1–5, 1998.

[15] H. E. Tseng and D. Hrovat, "State of the art survey: active and semi-active suspension control," *Vehicle system dynamics*, vol. 53, no. 7, pp. 1034–1062, 2015.

[16] M. Bär, *Vorausschauende Fahrwerkregelung zur Reduktion der auf die Insassen wirkenden Querbeschleunigung*. Forschungsgesellschaft Kraftfahrwesen GmbH Aachen (fka), 2014.

[17] Y. Zheng, B. Shyrokau, T. Keviczky, M. Al Sakka, and M. Dhaens, "Curve tilting with nonlinear model predictive control for enhancing motion comfort," *IEEE Transactions on Control Systems Technology*, early access, 2021.

[18] O. I. Kolev, "Thresholds for self-motion perception in roll without and with visual fixation target-the visual-vestibular interaction effect," *Functional neurology*, vol. 30, no. 2, pp. 99–104, 2015.

[19] Z. Lu, B. Shyrokau, B. Boulkroune, S. Van Aalst, and R. Happee, "Performance benchmark of state-of-the-art lateral path-following controllers," in *2018 IEEE 15th International Workshop on Advanced Motion Control (AMC)*. IEEE, 2018, pp. 541–546.

[20] B. Alrifaee and J. Maczijewski, "Real-time trajectory optimization for autonomous vehicle racing using sequential linearization," in *2018 IEEE Intelligent Vehicles Symposium (IV)*. IEEE, 2018, pp. 476–483.